Vibration Study of CoCrNi (Medium-Entropy Alloy) Gears for Marine Applications

M.Tech. Thesis

By
RASIKA PRAVIN KALOKHE

DEPARTMENT OF MECHANICAL ENGINEERING
INDIAN INSTITUTE OF TECHNOLOGY INDORE
MAY 2025

Vibration Study of CoCrNi (Medium-Entropy Alloy) Gears for Marine Applications

A THESIS

Submitted in partial fulfillment of the requirements for the award of the degree
of
Master of Technology

by
RASIKA PRAVIN KALOKHE

DEPARTMENT OF MECHANICAL ENGINEERING
INDIAN INSTITUTE OF TECHNOLOGY INDORE
MAY 2025

INDIAN INSTITUTE OF TECHNOLOGY INDORE

CANDIDATE'S DECLARATION

I hereby certify that the work which is being presented in the thesis entitled **Vibration Study of CoCrNi (Medium-Entropy Alloy) Gears for Marine Applications** in the partial fulfillment of the requirements for the award of the degree of **MASTER OF TECHNOLOGY** and submitted in the **DEPARTMENT OF MECHANICAL ENGINEERING, Indian Institute of Technology Indore**, is an authentic record of my own work carried out during the time period from July 2023 to May 2025 under the supervision of Dr. Dan Sathiaraj, Associate Professor, Department of Mechanical Engineering, IIT Indore and Prof. Anand Parey, Professor, Department of Mechanical Engineering, IIT Indore.

The matter presented in this thesis has not been submitted by me for the award of any other degree of this or any other institute.

11.06.25

Signature of the student with date
RASIKA PRAVIN KALOKHE

This is to certify that the above statement made by the candidate is correct to the best of our knowledge.

Signature of the Supervisor of M.Tech. thesis
Dr. Dan Sathiaraj

Signature of the Supervisor of M.Tech. thesis
Prof. Anand Parey

RASIKA PRAVIN KALOKHE has successfully given her M.Tech. Oral Examination held on **23rd May 2025**.

Signatures of Supervisors of M.Tech. thesis
Date: 9. 06. 2025

Convener, DPGC
Date:11-06-25

ACKNOWLEDGEMENTS

I would like to express my sincere gratitude to my supervisors, Dr. Dan Sathiaraj and Prof. Anand Parey, from the Department of Mechanical Engineering, for their invaluable guidance, helping me develop sound research intellect, inspiring curiosity, and for steering this research on the right path. Their expertise and encouragement have been instrumental in bringing this work to fruition.

I am grateful to IIT Indore's Sophisticated Instrumentation Centre team, for kindly allowing me to use their facilities and equipment throughout this project. Special thanks go to Mr. Sandeep Patil, Lab Manager, for his assistance with the Solid Mechanics Lab testing equipment, to Mr. Rajendra Goud, research scholar from the Advanced Metal Forming Lab, for his support with material characterization techniques, and to Mr. Santosh Yadav, research scholar from Vibration and Noise Control Lab, for his help with vibration-based measurements.

I would also like to thank the evaluation committee, Dr. Krishna Mohan Kumar, Dr. Indrasen Singh, and Dr. Mayank Chouksey, for their time, valuable suggestions, and constructive feedback.

I also thank my institute, IIT Indore, for providing a conducive academic environment and the resources necessary to carry out this research.

Finally, I am deeply thankful to my family, friends, and colleagues for their unwavering support and encouragement throughout this journey.

In loving memory of my Grandfather

Abstract

High strength gears find their applications in challenging conditions ranging from aviation engines, heavy-duty machinery, and deep-sea marine vehicles. Gears in marine vehicles must withstand extreme deep-sea pressure, a highly corrosive environment, and susceptance to wear. Given that maintenance is practically impossible at sea, surface treatments and coatings have been employed to improve the life of such gears. Such practices come with their own drawbacks of being expensive or not performing well under intense wear. Hence, need arises for innovating high strength marine gears in terms of the use of novel materials.

Medium Entropy Alloy, CoCrNi has captured researcher interest by its good strength-ductility synergy, high fracture toughness, high wear and corrosion resistance, without the formation of intermediate phases due to its stable single-phase FCC structure. Besides having properties that are consistent with the requirements for gear materials, the gears made of this alloy must also have less vibrations as compared to conventional marine gears to prevent the failure of gears by fatigue.

This thesis is the first work that manufactures equiatomic CoCrNi gears and compares their vibration characteristics with AISI 321 steel gears. Straight tooth spur gears are manufactured from a casted ingot using wire electrical discharge machining and then assembled with a setup to measure their vibration acceleration across a combination of different operating frequency and torque values by controlling the variable frequency drive and the magnetic break.

CoCrNi gears show a substantial decrease in the vibration. The root mean square values of the vibration acceleration from the time domain signal captured by the triaxial accelerometer show a 10 – 50 % decrease in the vibration strength of the signal in

axial, tangential, and radial directions. The deformation mechanisms present in CoCrNi, its twin dominated plasticity, strong work hardening behaviour, impart appreciable damping to the gears solidifying their application potential in high strength marine gearboxes.

Table of Contents

LIST OF FIGURES

LIST OF TABLES

ACRONYMS

AHSS	Advanced High Strength Steel
DP	Dual-phase
EDM	Electrical Discharge Machining
EDS	Energy Dispersive Spectroscopy
FCC	Face Centered Cubic
HEA	High-Entropy Alloy
MDL	Minimum Detection Limit
MEA	Medium-Entropy Alloy
SEM	Scanning Electron Microscopy
TRIP	Transformation Induced Plasticity
UTM	Universal Testing Machine

Chapter 1 Introduction

Gears are vital components of the mechanical engineering domain. They form the basis of mechanical systems that deal with precision in speed and torque control, power transmission, or motion transmission. Their variety has evolved over the years to cater to a wide range of requirements, from specific functionality to operating conditions.

1.1 High Strength Gears

With the onset of the early twenty-first century, gear manufacturing expanded to accommodate not only their geometric specifications, but also their functionality in terms of increasing power transmission capacity. Extremities in gear specifications have reached values like 100 mm of module, 150 m diameter, 100,000 kW power transmission capacity, rotational speeds of 100,000 rpm, and maximum circumferential velocity of 300 m/s [1]. Coupled with high operating speeds, high load carrying capacities, and presence in harsh environmental conditions, the categorization leads us to high strength gears.

1.1.1 Criticalities in Applications of High Strength Gears

i. **Spacecraft and Aviation Engines**

   Gears in aviation industries experience extremely dynamic thermal conditions during their operation. While accelerating from idle to full thrust, the temperature in the internal gears can rise to 300°C, levying exceedingly large thermal stresses on gears, their lubricants, and allied components. Consequently, in high altitude situations, or rapid descent, the temperature can drop as low as below -100°C that requires extensive surface treatment of the gears, and materials with large toughness that resist embrittlement at such low temperatures.

   For space applications, the pressure fluctuations around vehicles in near-earth orbits to deep space range from 10^{-4} – 10^{-7} Pa.

ii. Heavy duty machinery

In mining industry, or specialized construction equipment, gears must withstand large impact and load cycles generated due to rock crushing, excavating, and the vibrations due to excitation in such conditions at resonant frequencies. Needless to say, the bending fatigue developed on tooth roots causes rapid work-hardening and cracking at the root in extreme cases.

Constant exposure to abrasive particles causes damage to the tooth surface, and the downtime in highly commercial machinery such as these incurs immense loss.

iii. Marine Vehicles

In marine systems such as deep-sea submarines, structures must withstand pressures that rise to 200 – 300 MPa which is 2000 – 3000 times greater than atmospheric pressure because as the ocean depth increases, the pressure on transmission equipment also increases. A highly corrosive environment due to the salinity of the water, and increased susceptibility to pitting are additional challenges [[1].

Suitable surface treatments or coatings are used to counter these harsh operating conditions. Surface treatments mean an increase in the production cost of the gears. Moreover, as the gear teeth are continuously subjected to wear due to contact friction, the coatings have a chance of being scraped off, rendering them useless. Maintenance is practically impossible at sea, leaving one to look for other solutions to enhance gear reliability. In some cases, coatings may also put the gear steel at risk of hydrogen embrittlement which has been reported as a cause of catastrophic failure in steel structures.

1.2 Innovations in Gear Development

For developing gears that are suitable to operate in challenging conditions like the ones mentioned above and more, researchers have their own take on devising a solution fueled by their respective area of expertise.

1.2.1 Improvements in Gear Design

Besides choosing the appropriate type of gear as per the application, changes in design parameters, or conventional gear profiles is one of the routes to making high strength gears more effective. For example, the roost stress in polyoxymethylene gears can be reduced by 20%, and the bending fatigue life be increased by 30% by using S-shaped teeth [1]. Similarly, an increase in the pressure angle at the pitch line beyond 20° also raises the curvature of the tooth profile at the pitch line, decreasing the contact stresses. This, in turn, enables the gear to resist contact fatigue and bending fatigue more. Likewise, the overlap ratio during teeth meshing and the backlash provided, and numerous other parameters can be optimized to extend the load carrying capacity and performance life of the gear.

1.2.2 Advanced Manufacturing Techniques

Process parameters in the manufacturing methods of gears can be optimized to refine grain structure, diminish the requirement of surface treatment, enable in-situ alloying that is free from inclusions, all leading to gears with improved resistance to bending fatigue and longevity. Digital twins of such processes identify the nature of the end product in advance, facilitating a trial-and-error free, well theorized design of the manufacturing process to produce gears of suitable strength. With the invention of new manufacturing and machining techniques, manufacturers can produce gears with higher bending fatigue limits, superior contact fatigue resistance, improved core toughness, dimensional stability, and enhanced wear and scuffing resistance.

1.2.3 Novel Materials

Improving the bending fatigue limits and wear resistances of gear steels has had two approaches. In the first method, emphasis has been put on increasing the purity of metals and diminishing chances of inclusions that have been identified as one of the main causes of failure of gears due to fatigue. Secondly, the addition of different alloying elements and their impact on the mechanical properties of gear steels is being researched. Switching to a better material would relieve the pressure on expensive surface treatments altogether leading the path to revolutionize high strength gears. Incidentally, the medium entropy alloy being chosen in this study for a potential high strength gear material, has the same constituent elements cobalt, chromium, and nickel (Co,Cr,Ni) that are otherwise added to gear steel for enhancing its properties to adapt to challenging operating conditions.

1.3 Overview of Medium Entropy Alloys

To understand what are MEAs we must first look at High Entropy Alloys.

High Entropy Alloys

A high entropy alloy (HEA) is defined as an alloy with a large configurational entropy i.e. $\Delta S_{mix} > 1.5R$, where R is the universal gas constant (8.314 J/mol·K). ΔS_{mix} is defined as a quantity that measures the disorder associated with distributing different atomic entities across lattice sites. According to German physicist Rudolf Clausius, *'The entropy of the universe tends to a maximum'*. Hence, the increase in entropy is directly related to increased stability in systems.

The change in the configurational entropy of an alloy can be calculated as:

$$\Delta S_{mix} = -\mathrm{R}\sum_{i=1}^{N} c_i ln c_i$$

Where, R is the universal gas constant = 8.314 J/mol·K and

c_i is the mole fraction of element *i*.

It can be clearly concluded that ΔS_{mix} would be maximum for an equiatomic combination of alloying elements. Hence, the composition-based definition of HEAs states that it is an alloy in which multiple principal elements are mixed in equiatomic or near to equiatomic ratio of concentration. This increase in configurational entropy develops a stable single-phase microstructure which offers one with the luxury of a vast compositional space for designing new materials.

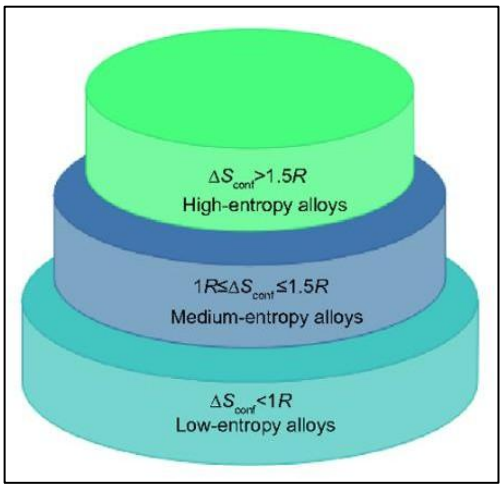

Figure 1 Classification of alloys based on configurational entropy (ΔSconf = ΔSmix) [20].

Medium Entropy Alloys

Similarly, Medium Entropy Alloys (MEAs) are alloys whose configurational entropy lies between 1R and 1.5R (with R having the same meaning as before). MEAs usually consist of three to four metallic elements. MEAs can be classified based on the purpose of their alloying as Structural MEAs (CoCrNi), Refractory MEAs (NbMoTaW), and Light-weight MEAs (containing Al, Ti, and Mg to reduce density).

Out of these, CoCrNi has shown promising mechanical properties such as an excellent strength-ductility synergy, and good fracture toughness even at cryogenic temperatures.

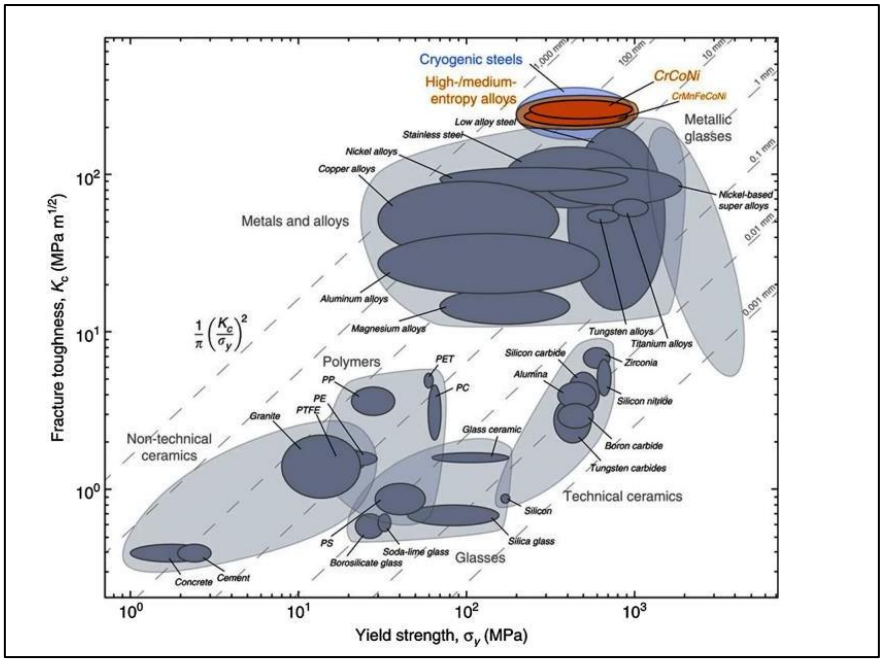

Figure 2 Ashby's bubble chart for fracture toughness versus yield strength of most damage tolerant materials at extremely low temperatures. CoCrNi clearly shows a good balance of both the properties as compared to others [21].

Although a direct comparison between the alloy with conventional materials is tricky due to the variety in their fabrication methods and difference in concentrations, it can still be noted from the bubble charts that CoCrNi shows an optimization of all the relevant mechanical properties that are best suited to their application in making gears.

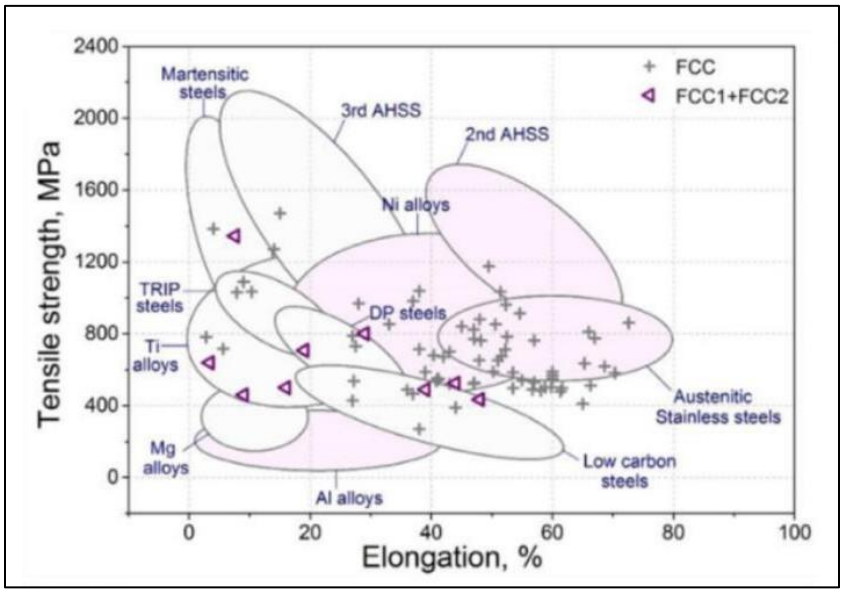

Figure 3 Ashby's bubble plot for tensile strength versus elongation of structural alloys and CoCrNi derived FCC MEAs [22].

1.4 Vibrations in Gears

Causes of Vibrations in Gears

Vibrations in a rigid body can be caused by any or all three main reasons. The change in magnitude of the excitation force acting at the same point in the same direction along the same line, the change in the direction of the exciting force acting with the same magnitude, at the same point, and along the same line, or the change in the line of application of the force of the same magnitude acting in the same direction.

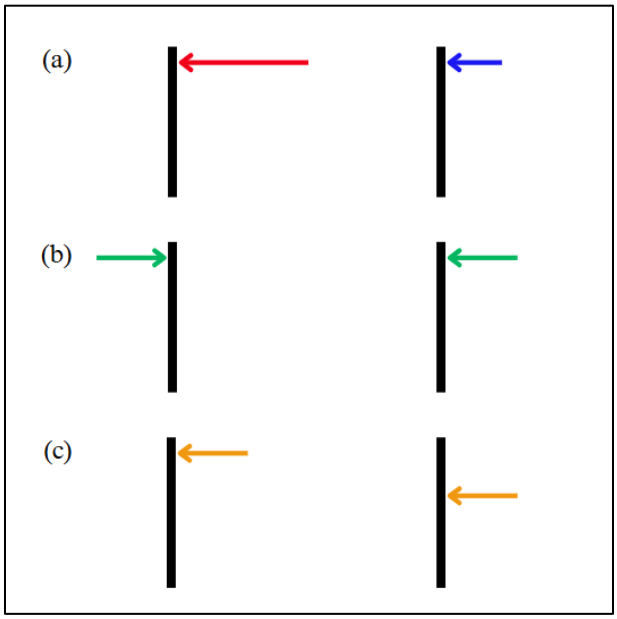

Figure 4 Vibration in a rigid body due to (a) change in magnitude of force, (b) change in the direction of force, (c) change in position of force [23].

Following the same principles, one can understand the cause of vibrations in gears particularly during meshing. To simplify the understanding, we can begin first by considering spur gears with an involute profile.

The force exerted on the tooth of the gear during mesh at the point of contact on the pitch line can be broken down into two components. The tangential component of the force here changes not only in magnitude but also in direction as the meshing progresses. This

generates vibrations in the gears at the gear mesh frequency for each cycle.

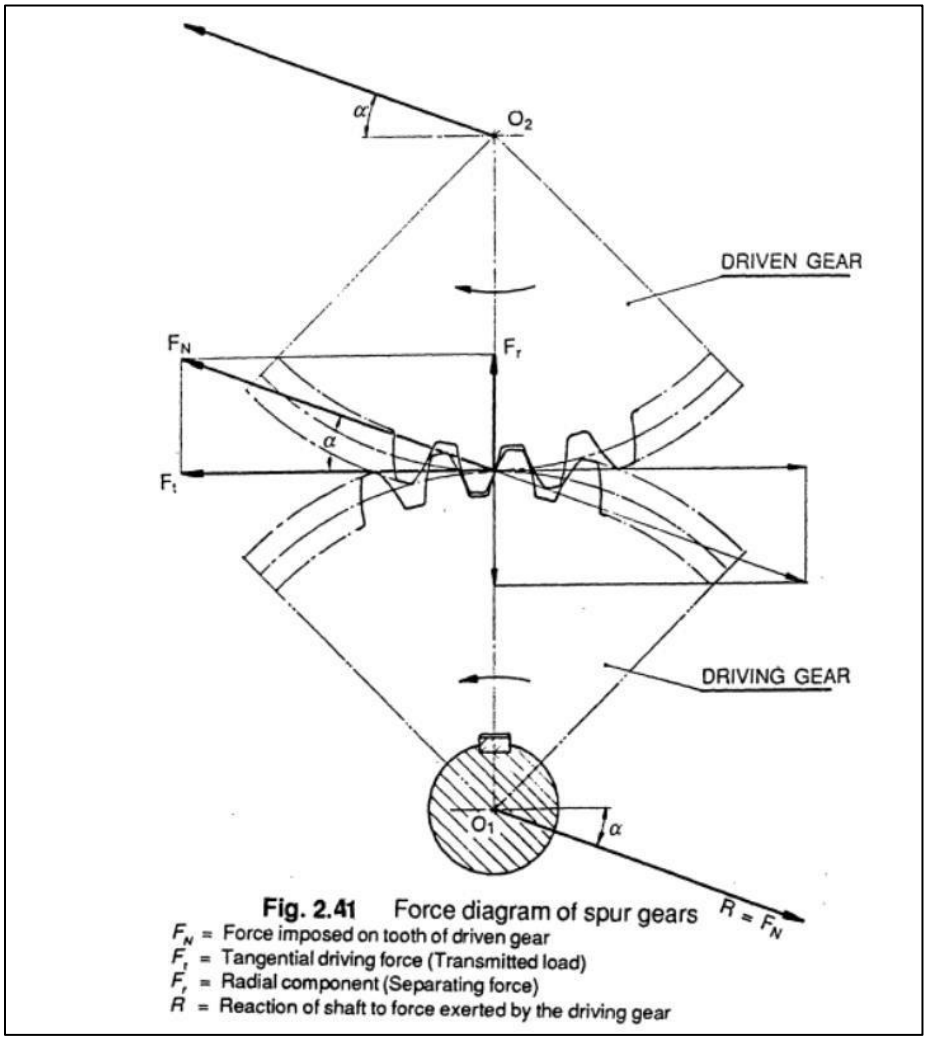

Figure 5 Forces acting on the gear teeth of spur gears during meshing [2].

When two gear teeth mesh under load, the transmitted torque generates tangential contact forces along the tooth flanks. As each pair of teeth comes into and out of engagement, these tangential forces rise and fall periodically, causing small elastic deflections in the gear body. Any mismatch between the applied force and the instantaneous mesh stiffness produces a transmission error which is essentially a tiny angular displacement between driving and driven gears. This error excites the gear's natural modes, sending torsional and bending waves through the shaft and housing. The result is a cyclical vibration at the

gear-mesh frequency and its harmonics whose amplitude depends on torque level, tooth profile accuracy, and material damping. In practice, these forces manifest as audible noise and contribute to fatigue at the tooth root.

Root Mean Square (RMS) Value of Vibration Acceleration

For the purpose of this study, we will consider all the gear vibrations to be either in the radial, axial, or transverse direction. This is to maintain consistency with our vibration measurement methods i.e. measurement of gear vibrations using a triaxial accelerometer which has been described in detail in the 'Experimental Vibration Analysis' section of this thesis.

The RMS value of a vibration signal is a single-number metric that represents the signal's effective energy over a given time window. Mathematically, for a discrete time-series of vibration samples x_i (like acceleration in mm/s²) taken at a constant sampling interval, the RMS is defined as:

$$RMS = \sqrt{\frac{1}{N}\sum_{i=1}^{N} x_i^2}$$

Where, N is the total number of data points.

Significance of RMS in Gear Vibration Analysis

RMS of the vibration acceleration of the gear pair:

i. **represents the overall vibration energy:** RMS condenses a complex waveform that is comprising many mesh-frequency oscillations, harmonics, and random noise into one value that correlates with the total vibratory energy transmitted through the gear and its housing.

ii. **is insensitive to sign and phase:** As vibrations oscillate above and below zero, a simple average

would add up to give zero. RMS, by using squared values, captures both positive and negative excursions equally, ensuring that the measurement reflects true vibrational intensity.

iii. **correlates with fatigue stress:** Since alternating stress in a gear tooth root is proportional to acceleration, higher RMS acceleration implies higher cyclic bending force. Over many cycles, this raises the risk of fatigue crack initiation. Monitoring RMS allows engineers to track the load-severity trend rather than just intermittent peaks.

iv. **is robust to random noise** While spikes or singular impacts influence peak values heavily, RMS 'smoothens' their effect since it integrates energy over a time duration. This makes RMS a more stable indicator of ongoing conditions like gradual wear or misalignment than instantaneous peak-peak readings.

Thus, a consistently lower RMS for one material of gears against another under identical speed and load directly indicates reduced dynamic forces and better damping.

1.4.3 Minimizing Gear Vibrations to Boost Longevity

In addition to producing gears suitable for heavy duty applications, minimizing vibration in such gears is critical for extending gear lifespan because each oscillation under load generates micro-stresses that accelerate fatigue and surface damage. In marine environments, these are compounded by corrosive seawater and particulate contamination, making conventional steels prone to pitting, wear, and crack initiation. A novel gear material that inherently produces lower vibration amplitudes due to higher stiffness and internal damping, significantly reduces cyclic stress peaks at the tooth roots. This reduction in dynamic loading delays fatigue crack nucleation and

propagation, resulting in smoother operation and fewer unexpected failures.

Moreover, if this material also exhibits excellent wear and corrosion resistance, it addresses two other primary causes of marine-gear degradation. High wear resistance preserves gear geometry and backlash settings over long duty cycles, while superior corrosion resistance prevents chloride-induced pitting and stress-corrosion cracking. When vibration is low, lubricating films remain more stable, further decreasing wear rates. Taken together, a gear alloy combining reduced vibrational excitation with robust surface durability and anti-corrosive properties becomes an ideal choice for marine applications. It ensures quieter, more efficient propulsion systems, reduces maintenance intervals, and ultimately delivers longer service life in the challenging conditions of saltwater exposure and heavy cyclic loads.

1.6 Organization of the Thesis

Chapter 1 provides an overview of the dependance of mechanical systems on high strength gears, discussing their applications, and singling out marine systems as the chosen topic of concern. Discussions have been made regarding ways to enhance such gears, and how the choice of novel material reducing overall gear vibrations while adhering to other boundary conditions would be a good solution.

It also sheds light on the evolution of HEAs as advanced materials and narrowing the focus on MEAs as they bridge the gap between the former and conventional alloys. Reasons for CoCrNi being a representative MEA and of particular interest for the current study by aligning its properties with that of gears have been elaborated.

The chapter outlines the causes and effects of vibrations in gears and explains why the mitigation of such vibrations would lead to increased fatigue life of gears. The same aspects have been discussed with respect to marine gears in particular, for realizing the significance of the objectives of this research.

Chapter 2 explores the issues with marine gear failures recorded in the archives and how CoCrNi would be a good choice of material for those. After highlighting gaps in the research for structural applications of CoCrNi, the chapter ends in finalizing key objectives that will govern this research.

Chapter 3 is an in-depth description of the methodology used in this research. The process of developing high strength gears from scratch, right from developing the material itself to producing the finished gears, has been illustrated. The chapter also provides a detailed account of the experimental route followed for material testing and benchmarking, and the subsequent steps for a comparative vibration study of CoCrNi and AISI 321 gears. As the experimental set-up has been prepared in-house, necessary details regarding its construction and operating procedure have been mentioned.

Chapter 4 discusses the results obtained from the aforementioned experimentation and inferences that can be drawn from those with regards to proposing CoCrNi as a suitable material for high strength marine gears. The results from the material characterization and mechanical properties characterization have been correlated to the vibration performance of the CoCrNi gears in order to provide a fitting basis for the study.

Chapter 5 summarizes the results and their inferences while concluding the thesis with a call back to the prescribed objectives. The chapter also provides motivation and directions to the future scope of this work that can be explored by upcoming researchers.

Chapter 2 Formulation of Problem Statement

Gears in marine applications must contend with extreme environments; corrosive saltwater, heavy cyclic loads, and stringent reliability requirements; yet conventional steel alloys often succumb to pitting, wear, and fatigue under these conditions. Despite advances in surface treatments and lubrication, vibration-induced stresses continue to initiate microcracks and accelerate gear failure. This chapter formulates the core problem: identifying an alloy system that simultaneously offers superior corrosion and wear resistance while minimizing dynamic excitation to extend gear service life. By articulating this challenge, we establish the foundation for investigating how novel materials, such as CoCrNi medium-entropy alloys, can address these critical shortcomings.

2.1 Literature Survey

2.1.1 Archives of Failure in Marine Gears

Wu et al. (2024) report that deep-sea environments impose hydrostatic pressures up to 200–300 MPa on gear housings, necessitating materials with high yield strength and structural integrity at deep sea level. In addition, exposure to chloride-rich seawater accelerates pitting corrosion and stress-corrosion cracking; alloys or coatings must therefore exhibit excellent passivation and resistance to localized attack [1].

A flywheel gear made from case-hardened AISI 1055 steel (with hardness values for the core and case being ~198 HV and ~559 HV respectively) was investigated, that failed when a sudden throttle surge imposed an inertial overload torque, generating von Mises stresses equal to 737 MPa that were well above the material's yield strength of 550 MPa. The crack was initiated at the high-stress root fillet in the case layer and propagated through the core, leading the authors to recommend tighter engine-operation controls to prevent such overloads [3]. An earlier study of a container-ship engine analyzed two fractures:

the gearbox shaft (made of SAE 4340 alloy steel) failed by rotational-bending fatigue at a sharp notch due to insufficient endurance strength, while the clutch shaft (made of SAE 5046H carbon steel) fractured torsionally after pitting corrosion weakened the surface under moisture-contaminated lubricant [4].

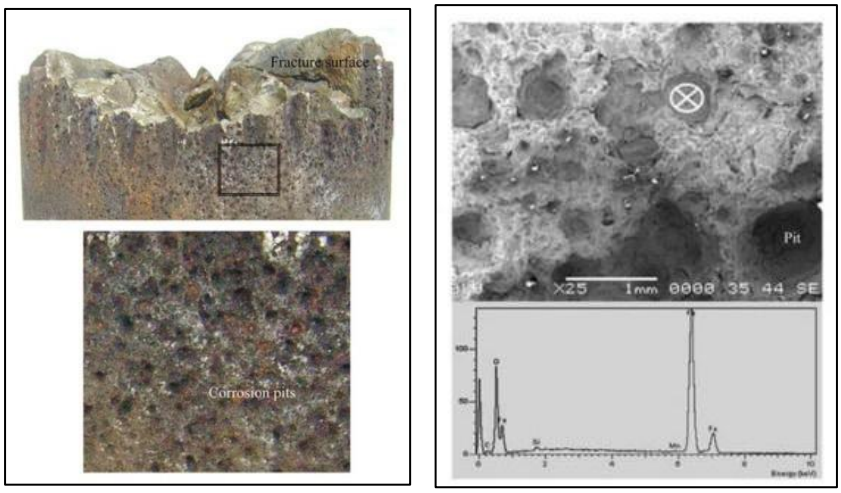

Figure 6 SEM images and EDS plots of fractured surface of marine gear tooth showing corrosion pits. The presence of iron and oxygen peaks in the EDS plot clearly denotes that the pits show corroded area and not simple voids [4].

As a solution to avoid such failures in the future, they proposed tougher, deep-hardened alloys for the gearbox shaft and the use of improved lubrication or a higher-alloy steel to mitigate corrosion on the clutch shaft. Using vibration-signature analysis for diagnosis on a high-speed marine gearbox, commonly employing carburizing steels such as 20CrMnTi, broken-tooth failures were attributed to high-cycle contact fatigue under dynamic loading [5] . They recommended online vibration monitoring algorithms to detect incipient cracks before catastrophic tooth loss. Assuming typical quenched and tempered alloy steels, nonlinear vibration phenomena in a marine gearbox were modeled, showing that misalignment, nonlinear mesh stiffness, and bearing support flexibility can excite subharmonic and chaotic oscillations that accelerate fatigue crack growth [6]. Their solution emphasized precise gear-mesh alignment, optimized profile modifications, and appropriately stiff bearing supports to suppress these destructive resonances.

Fractographic analysis archives of marine gearbox components show that corrosion, presence of inclusions, and vibrations associated with gears lead to fatigue failure of such components [3], [4], [7]. It is important to note that steels used in making such components as recorded in the studies contain Cr, and Ni in varied quantities as the alloying elements which are also the constituent elements of the MEA we propose should be used instead.

2.1.2 Review of CoCrNi

CoCrNi has been extensively studied in terms of its different fabrication approaches and the exploration of properties imparted to the material due to said approach. In broad terms, the phase stability, high work hardening through twinning, and low stacking fault energy of the alloy gives it exceptional damage tolerance [8] [9]. Low SFE will exhibit strong in-service strain hardening at tooth root delaying fatigue crack initiation. Cold rolling, coupled with annealing produces ultrafine grain structure in the alloy giving it a UTS of 1.15 GPa while retaining its ductility [10]. Molecular dynamics simulations have also been performed to investigate atomistic sources of high hardness and twin formation that contribute to the macroscopic strength of the alloy [11]. This would lead to excellent resistance to contact fatigue on tooth flanks, reducing pitting and scuffing.

A summary of the properties exhibited by CoCrNi found across literature through various fabrication routes along with the properties of different marine grade steels have been provided in Table 1. The table clearly shows how CoCrNi compares with conventional marine gear materials for ease of judging its application feasibility. It also gives a choice of reference material that can be chosen in order to perform comparative mechanical property and vibration analysis between gear pairs of different materials.

Table 1 Mechanical properties comparison of CoCrNi and marine grade steels.

Material and Fabrication Route	0.2 % YS (MPa)	UTS (MPa)	ε_f (%)	Hardness	Ref.
CoCrNi					
CoCrNi: **1.Molten-salt electrolysis** **2.Arc-melt**	366	695	40	253 HV	[12]
CoCrNi: **1.Molten-salt electrolysis** **2.Arc-melt** **3.Cold-roll 60 %** **4.Anneal 800 °C for 1 h**	994	1183	14	412 HV	[12]
CoCrNi: **1. Vacuum-arc melt** **2. Suction cast** **3. Homogenize 900 °C for 2 h** **4.Water-quench** **5. Cold-roll 50 %** **6. Recrystallize at 1200 °C for 2 hours**	430	800–880	73	198 HV	[8], [13]
Marine Grade Steels					
Standard annealed AISI 316	205	520	40	187 HB ≈ 196 HV	[14]
Standard annealed AISI 321 (Reference gear material)	205	515	40	217 HB ≈ 222 HV	[15]

2.2 Research Gap

i. Though CoCrNi has been extensively studied for its potential as a coating for components working in harsh environments, its use as a structural material is yet to be explored.

ii. The correlation between known properties of CoCrNi with that of the requirements for high strength gears in general, and marine gears in particular is missing in the literature.

iii. Consequently, there are no records of gears being developed from CoCrNi, and neither have the vibration characteristics of such gears been studied.

iv. The effect of vibration on components made of HEAs or MEAs has not been analyzed.

2.3 Objectives of the Research

i. Understanding the deformation characteristics in CoCrNi coupled with those of high strength gears to classify it as a suitable material for the same.

ii. Manufacturing CoCrNi gears and performing comparative experimental analysis of vibration acceleration with reference material gear.

iii. Choosing a suitable material for manufacturing reference gears that would closely mimic marine gears in operation.

iv. Drawing inferences about the vibration performance of CoCrNi gears based on metallurgical findings that have been reported by researchers.

Chapter 3 Methodology

3.1 Fabrication of CoCrNi

As discussed in Chapter 2, various methods for the fabrication of CoCrNi have been explored by researchers. It is also important to note that the choice of method of fabrication of the alloy would also depend upon its end application. Additive manufacturing processes such as LPBF, powder metallurgy, and WAAM have been reported to deliver slightly porous samples of CoCrNi. For the subsequent manufacture of the alloy into gears, the raw material should be obtained in bulk, and must be free from any inclusions, porosities, or other irregularities within the material that would act as stress concentration sites as gears are structural components that take heavy static and dynamic loads. In such a scenario, casting proves to be an effective solution.

A casted ingot of 64 mm x 96 mm x 40 mm was obtained by melting Co, Cr, Ni lumps of roughly equal weight. The parameters used for the induction casting of the alloy have been given below.

Table 2 Process parameters used to fabricate CoCrNi in an induction furnace through casting.

Parameter	**Value**
Furnace Power	30 – 50 kW
Melting temperature	1500°C, above the CoCrNi liquidus temperature for complete melting
Crucible Material	MgO-lined graphite
Atmosphere	Argon with 99.999 % purity at 0.1 - 0.2 bar overpressure
Hold Time	5-10 minutes at melt temperature, under stirring
Pouring temperature	≈1500°C, and slightly below melting temperature to minimize oxidation
Cooling rate	Air cooled

The cast was remelted 5 times to ensure homogeneous mixing and stirred electromagnetically. A 2kg ingot was obtained after solidification.

Figure 7 As-cast ingot of CoCrNi.

3.2 Material Testing and Characterization

A detailed analysis of the sourced material was performed before proceeding for further experimentation. Testing was also done after subjecting the material to heat treatment.

3.2.1 EDS Mapping of CoCrNi for Composition Verification

The validation of the material in terms of elemental composition and homogeneity was performed using the Energy Dispersive Spectroscopy (EDS) technique. A 10 mm x 10 mm x 5 mm sample was cut from the corner of the casted block using wire EDM. The sample was cold mounted using a mold. Then it was polished using polish papers with the grade becoming progressively finer and using diamond paste on a polishing cloth for achieving the final mirror-like finish to obtain a deformation free, reflective surface.

EDS of prepared sample was performed using FE – SEM Supra 55 by Zeiss.

3.2.2 Tensile and Microhardness Testing

The same sample used for the EDS analysis was taken for microhardness testing. A mirror finish is required for clear visualization of the indentation. A similar sample was prepared from

the heat treated CoCrNi sample. A hot mounted sample is preferred for microhardness testing as it ensures a flat base.

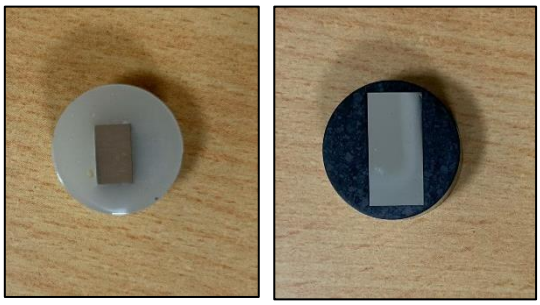

Figure 8 Specimens prepared for microhardness test by cutting the sample using wire EDM and polishing with SiC paper from grit size 600 to 3000 until a mirror-like finish is obtained.

A sub-size tensile test specimen was cut from the as-cast alloy using wire EDM as per ASTM E8 which has been employed previously in the research revolving around MEAs [16]. Its thickness was 1.2 mm and the width at the gauge length was 1.52 mm. The sample was loaded in the UTM and tested at a strain rate or crosshead speed of 1 mm/min.

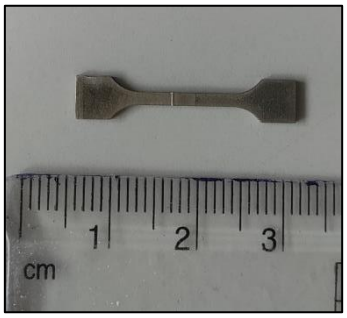

Figure 9 Sub-size tensile test specimen tested using UTM at a strain rate of 1mm/min.

3.3 Manufacture of CoCrNi gears

The gear dimensions were finalized after considering the constraints posed by the experimental test set-up available. The dimensions had to be chosen in such a way that the bore diameter was 14 mm, the distance between the centers of the driving and the driven shaft was 100 mm, the distance of the shafts from the base of the set-up would accommodate the gear, and the outermost path of the gear profile to be

cut from the blank would leave an excess material of 5 mm around its path so that the blank could be held on the wire EDM machine as was the requirement of the manufacturing equipment.

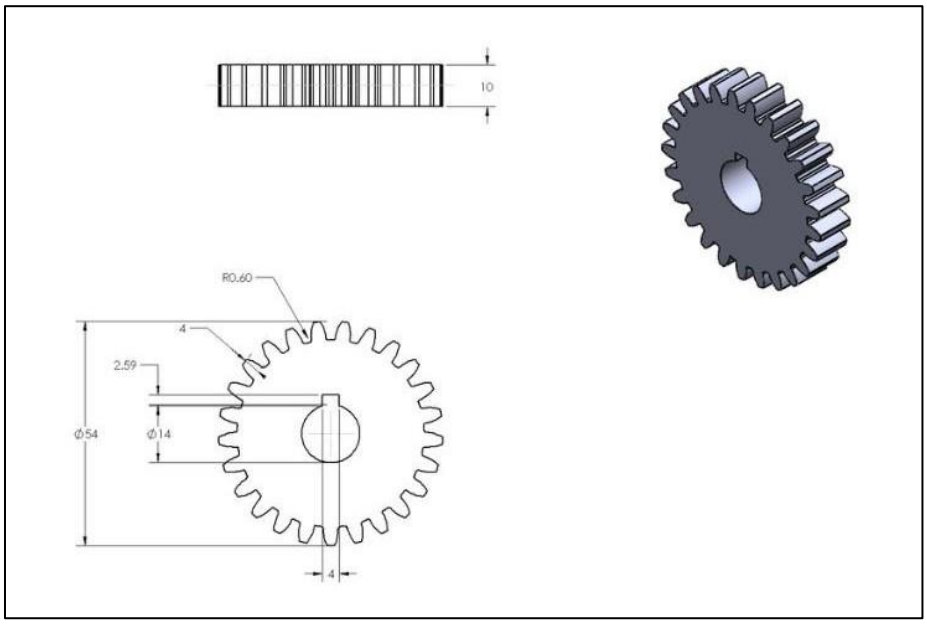

Figure 10 Drafting of gear model to conform with the experimental set-up.

Table 3 Specifications of the straight tooth spur gear with involute profile.

Specification	**Value**
Number of Teeth	25
Module	2 mm
Pitch Circle Diameter	50 mm
Face Width	10 mm
Bore Diameter	14 mm
Outer Diameter	54 mm

The slot for the keyway shown in Figure 10 was designed as per the dimensions of the key on the test set-up. The gear was modelled and the '.dxf' file of the front view was uploaded to the machine for gear cutting. Wire EDM was chosen as the preferred method of manufacturing the gears as it can provide a good surface finish and leaves no residual stresses due to machining in the finished workpiece.

Moreover, as our requirement was to manufacture a single pair as opposed to mass production, wire EDM would not require any additional tooling to be customized as per our design. The wire EDM machine used was Electronica Hi-Tech Job Master D-zire with the cutting tool being a brass wire of Ø 0.25 mm and the machine having 10 µm accuracy. The alloy was first parted at 10 mm thickness (the face width of the gear) and then each gear cut from a blank individually.

Figure 11 Gears manufactured using wire EDM.

The gears were then heat treated in a furnace by heating up to 1000°C for 2 hours in an Argon rich environment and allowed to cool naturally. The presence of Argon prevented any of the constituent elements of the alloy from oxidizing.

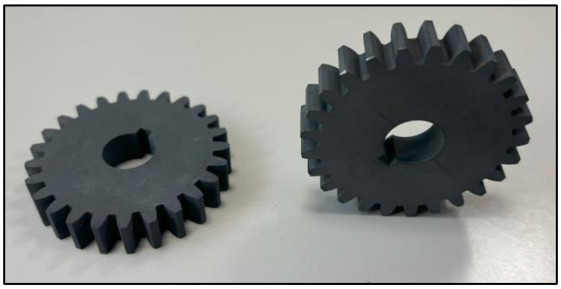

Figure 12 Gears post heat treatment at 1000°C in an Argon based environment.

An identical set of gears was manufactured from AISI 321 using the same manufacturing method to ensure that the comparison between the

vibration signals of both the sets of gears would not be influenced by other parameters.

3.4 Experimental Vibration Analysis

The experimental set-up was equipped with components to help analyze the behavior of the gears across a wide range of frequencies of operation and loads in the form of torque.

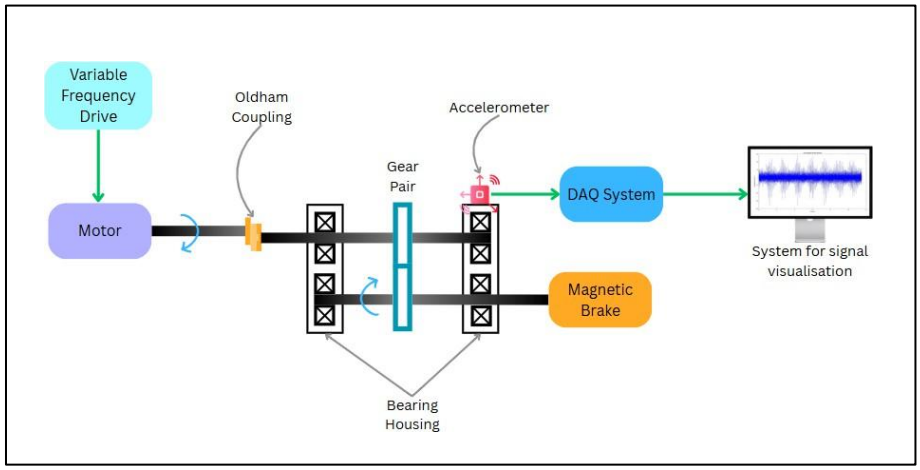

Figure 13 Schematic diagram of the experimental test set-up.

3.4.1 Test Rig Components and Arrangement

The nature and function of each component is as follows:

1. Variable Frequency Drive (VFD): It can drive the motor at a desired frequency, which in turn is imparted to the gears, to gain control over experimental parameters.
2. AC Motor: It is the prime mover that drives the input shaft.
3. Oldham Coupling: Its function is to eliminate any misalignment that may be present in the coupled input shaft, thereby nullifying vibrations in the setup due to such misalignment.
4. Gear Pair: The desired pair of gears to be studied which in this case are straight tooth spur gears with an involute profile.
5. Triaxial Accelerometer: The PCB Piezotronics accelerometer is a vibration sensor that measures vibration acceleration in the X, Y, and Z axes simultaneously.
6. Magnetic Break: It helps to vary the load on the driven shaft by allowing the application of desirable torque.

7. Bearing Housing: It contains ball bearings which bear the shafts. Two bearing housings are required in the setup to support the shafts on either end. The housing also proves important in terms of providing a platform for mounting the accelerometer while conducting the experiment.
8. Data Acquisition System (DAQ): The four channel DAQ collects data from the accelerometer and sends it to the system for display.
9. System: A laptop with the NVGate software installed helps with the visualization and analysis of the signal as per the requirements of the user.

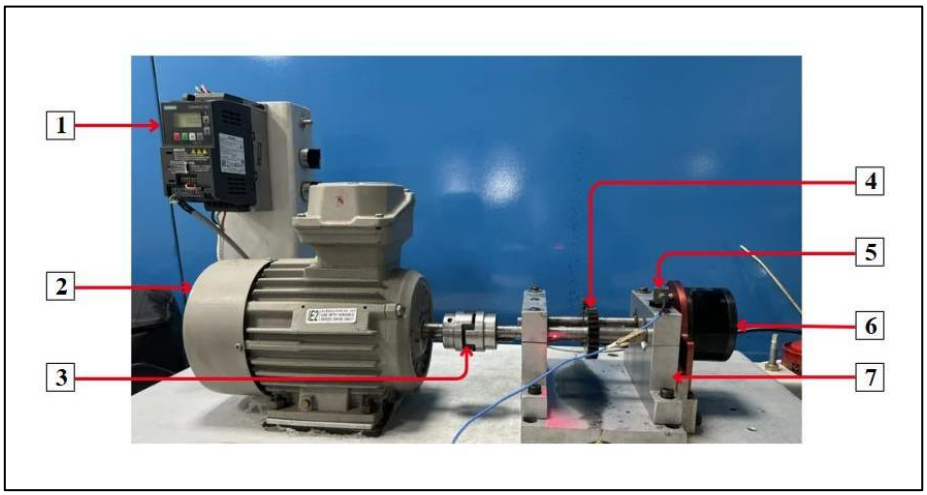

Figure 14 Experimental test set-up used for measuring gear vibrations.

Figure 15 Triaxial accelerometer (225948) by PCB Piezotronics with sensitivities (in mV/g) in X, Y, and Z axes 50.3, 47.6, and 47.8 respectively.

Figure 16 Data Acquisition system by OROS.

3.4.2 Experimental Procedure

The pair of CoCrNi gears was first assembled with the setup. The two halves of the bearing housing lay on top of each other, which were screwed together. Removing the top half allowed for the easy removal of shaft from the housing. The bearing was removed from the shaft using a bearing puller. CoCrNi gears were assembled, one each on the driving and the driven shaft. The bearing housing was closed after assembling the gears. The accelerometer was placed on the bearing housing with the help of wax that comes with the sensor. This adhered the sensor firmly to the housing. The orientation of the sensor was noted in order to replicate it while taking readings with another gear pair for comparison. This is necessary because we need the acceleration data for a particular axis for both the gear pairs to be in the same direction. The sensor was connected to the DAQ system. The DAQ system was connected to the laptop. The laptop, DAQ system, and the setup were all connected to the power source. The NVGate software was configured using details like the sensitivity of the accelerometer (provided with the equipment manual), the sampling frequency (here, 12,800 Hz), and which channel of the DAQ system showed the vibration acceleration for X, Y, and Z, respectively.

The setup was then run at 5 Hz, 10 Hz, and 15 Hz frequency, while varying the torque as 0 Nm, 0.5 Nm, and 1 Nm with each frequency and the data for all three axes was captured, thus giving data points for twenty-seven different time domain scenarios. Each signal was captured for approximately 10 seconds.

The entire procedure was then repeated for the AISI 321 gear pair, which is our reference gear pair.

The data was extracted from the NVGate software using a key provided with the equipment, in '.txt' format. The time domain plots for all the iterations were generated using a Matlab code.

The RMS plots for all the signals were constructed for a comparative study.

Chapter 4 Results

4.1 Material Characterization Findings

The EDS analysis of the polished specimen shows a near-equiatomic concentration of all the constituent elements.

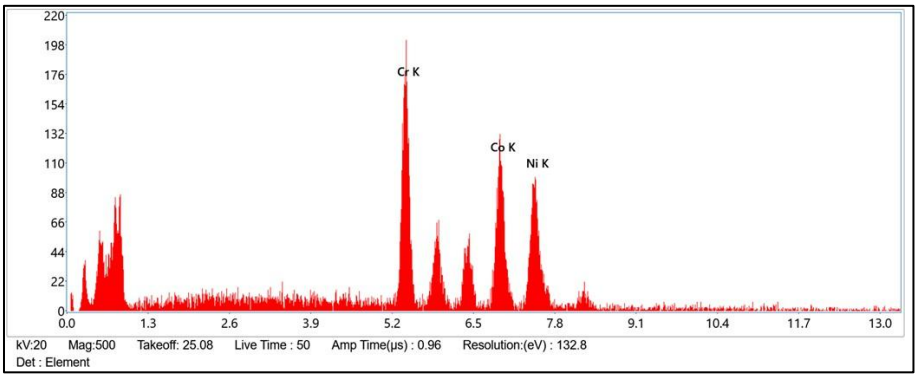

Figure 14 EDS plot of as-cast CoCrNi sample for source material authentication.

The higher peak of Cr shows a marginally greater contribution of the element in the alloy.

Table 4 EDS results of the as-cast CoCrNi sample for authentication of the source material.

eZAF Quant Result - Analysis Uncertainty: 6.77 %				
Element	**Weight %**	**MDL**	**Atomic %**	**Error %**
Cr K	28.2	3.11	30.7	5.5
Co K	37.2	1.83	35.8	7.2
Ni K	34.7	2.96	33.5	7.1

As all the obtained values of concentrations are below their respective MDL (Minimum Detection Limit), the result can be trusted, and the material be considered for further downstream processing that is a part of the research.

The sub-size tensile specimen was loaded up to failure and the following plot was obtained from the generated data points. The curve mimics the nature of plots obtained for the tensile testing of CoCrNi as recorded in the literature.

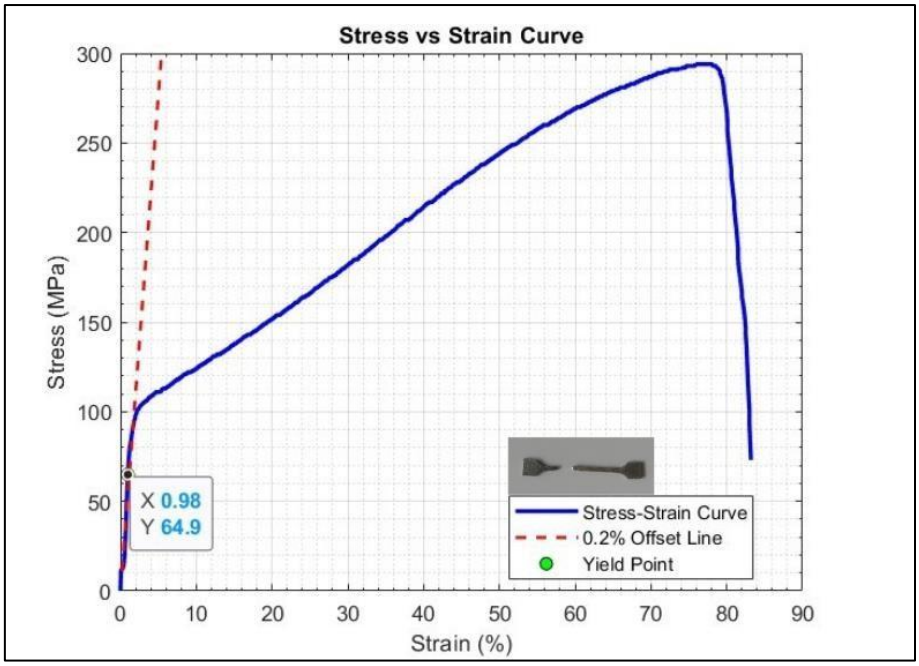

Figure 15 Stress (MPa) versus strain (%) curve obtained on the tensile testing of sub-size specimen at 1mm/min strain rate.

The curve obtained clearly shows that CoCrNi exhibits strong work hardening behavior as seen in the literature [2]. The Ultimate Tensile Strength was found to be 294 MPa and the elongation up to fracture was 82.1%. The 0.2 % Yield Strength was 64.9 MPa.

The region of the graph before the yield point gives an Elastic Modulus of 235 GPa. The drop in the slope of the curve after yield, with a gentler rise, denotes the work hardening behavior of the alloy which has been attributed to the solid solution strengthening and twin formation [3]. The area under this curve showcases the fracture toughness of the alloy, implying that it is capable of absorbing large amounts of energy before failure. It is also representative of the excellent strength-ductility synergy of CoCrNi that is one of the main characteristics of this alloy that has attracted researchers' interest [19].

The sharp drop in stress beyond the highest point in the graph implies that the material is no longer capable of bearing the stress beyond the ultimate tensile strength and the crack is quick to form and propagate leading to the failure of the material.

4.2 CoCrNi and AISI 321 Gear Vibration Comparison

The following data has been obtained after executing the method described in section 5.4.2 of the previous chapter. Inferences have been drawn based on the direct comparison between time domain signals of the two gear pairs of different materials, and an overview of the RMS values of vibration acceleration of the two kinds of signals for better understanding of the signal strength.

4.2.1 Time Domain Signal Analysis

The time domain plots for different cases for both the gear pairs have been given below for comparison.

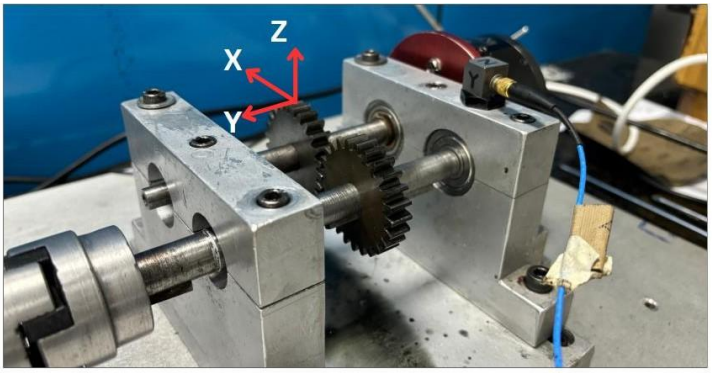

Figure 16 X-axis denotes the radial direction, Y-axis denotes the axial direction, and Z-axis denotes the tangential direction.

Time domain signals of CoCrNi gears

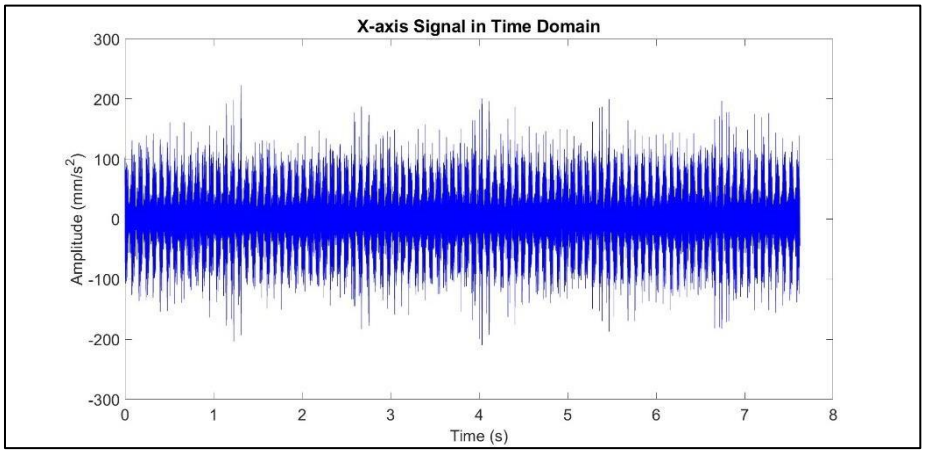

Figure 17 X-axis vibration acceleration time domain signal of CoCrNi gears at 15 Hz operating frequency and 1 Nm torque.

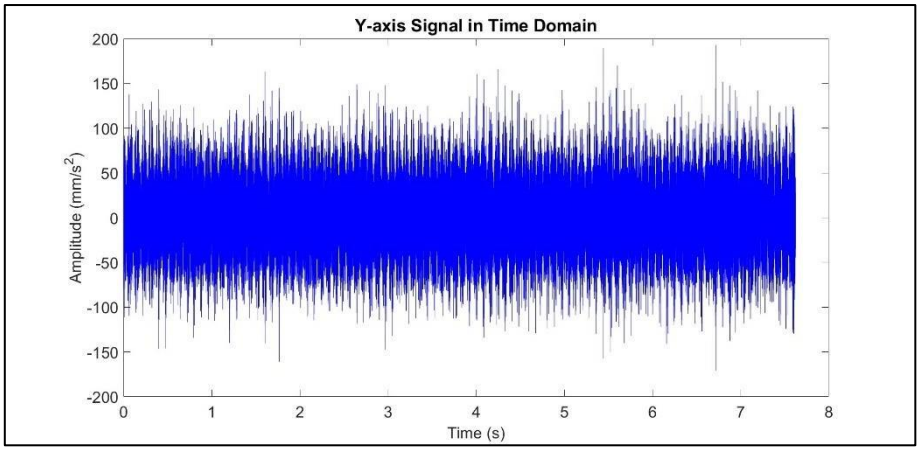

Figure 19 Y-axis vibration acceleration time domain signal of CoCrNi gears at 15 Hz operating frequency and 1 Nm torque.

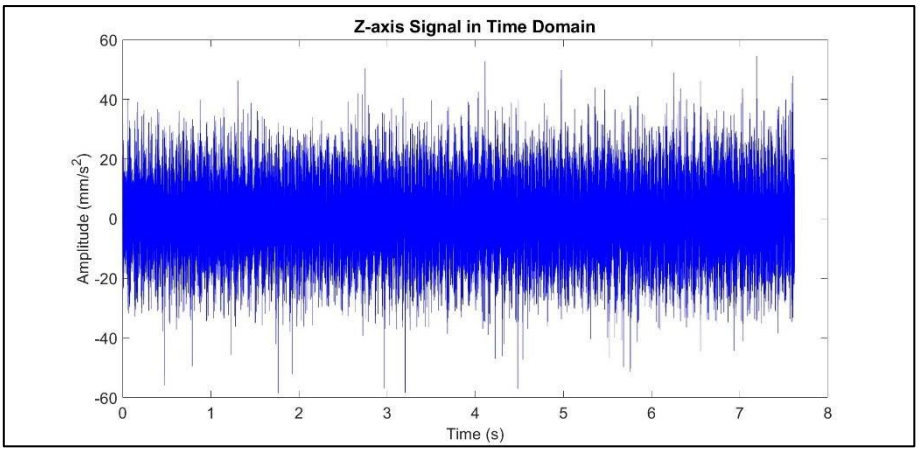

Figure 18 Z-axis vibration acceleration time domain signal of CoCrNi gears at 15 Hz operating frequency and 1 Nm torque.

Time domain signals of AISI 321 gears

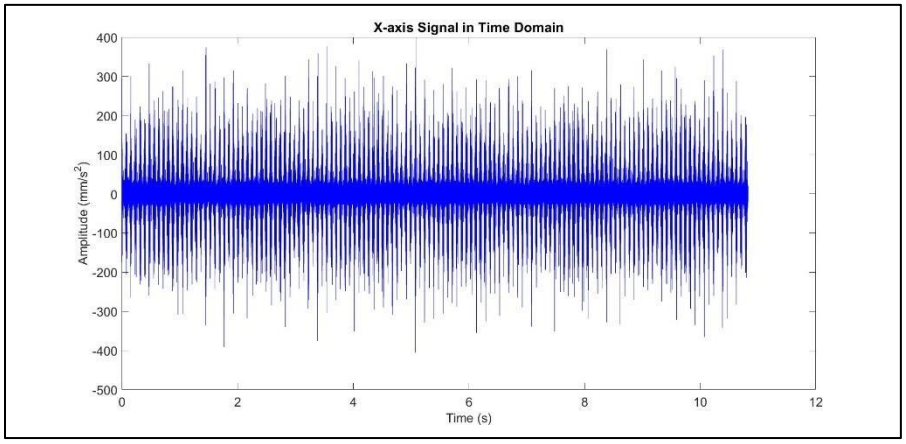

Figure 20 X-axis vibration acceleration time domain signal of AISI 321 gears at 15 Hz operating frequency and 1 Nm torque.

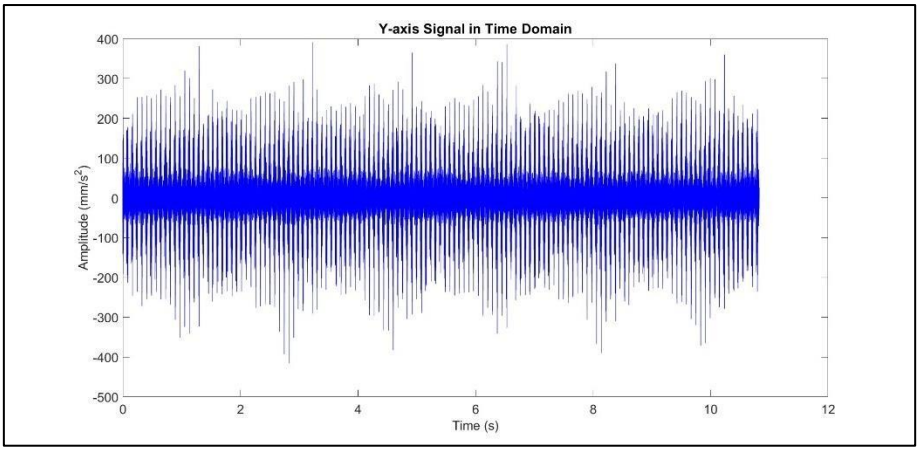

Figure 21 Y-axis vibration acceleration time domain signal of AISI gears at 15 Hz operating frequency and 1 Nm torque.

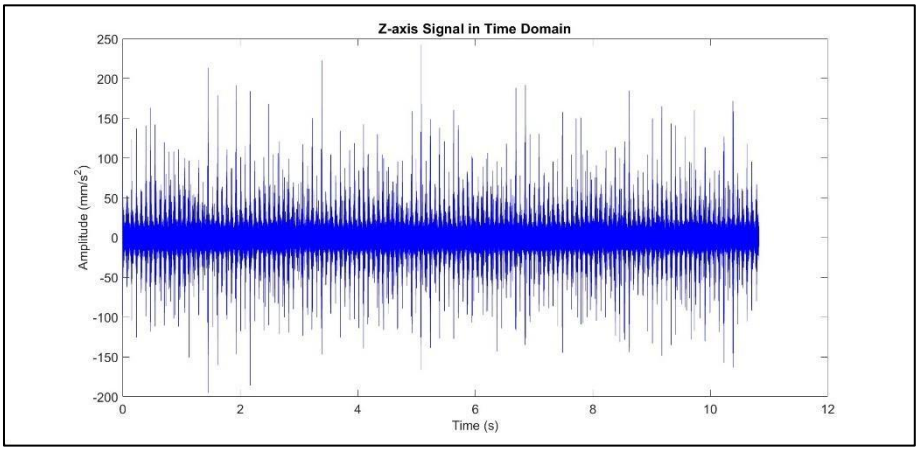

Figure 22 Z-axis vibration acceleration time domain signal of AISI gears at 15 Hz operating frequency and 1 Nm torque.

The six time-domain plots at 15 Hz and 1 Nm clearly show that CoCrNi gears produce substantially lower vibration amplitudes than AISI 321 under the same operating conditions. In each direction; tangential (Z), radial (X), and axial (Y); CoCrNi's peak-to-peak accelerations are roughly 40 %–80 % smaller than those of AISI 321. For example, along the X-axis CoCrNi's oscillations reach about ±220 mm/s² (≈ 440 mm/s² peak-to-peak), whereas AISI 321's reach ±380 mm/s² (≈ 760 mm/s² peak-to-peak). These smaller force spikes directly translate into lower accelerations recorded by the housing-mounted accelerometer.

4.2.2 Vibration RMS Comparison

The RMS values of vibration acceleration have been compared for CoCrNi and AISI 321 gears.

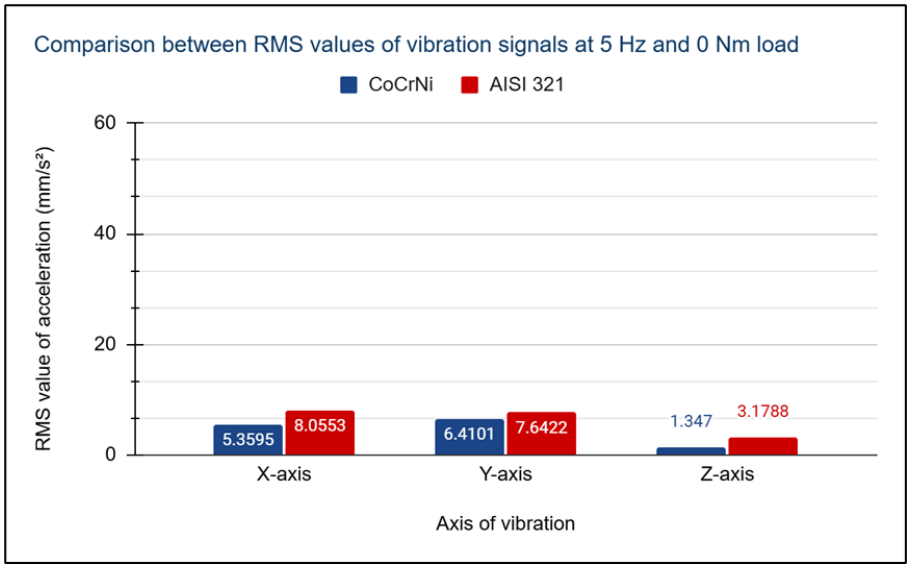

Figure 23 Comparison between RMS values of vibration signals at 5 Hz and 0 Nm.

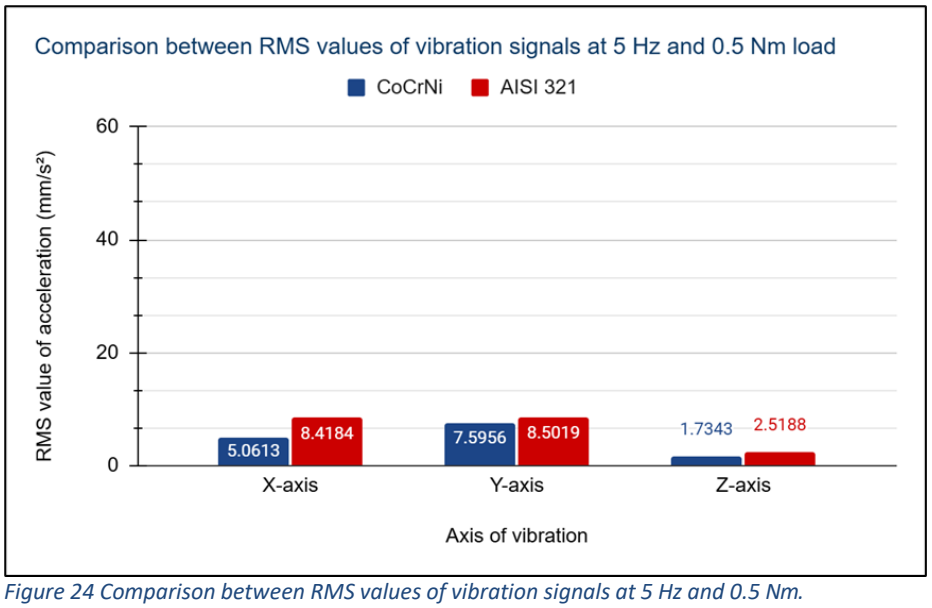

Figure 24 Comparison between RMS values of vibration signals at 5 Hz and 0.5 Nm.

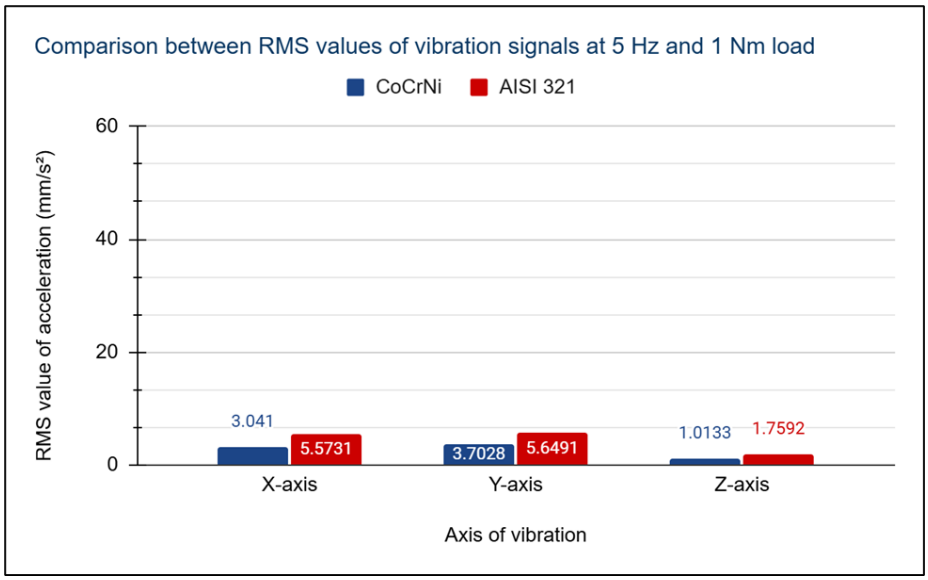

Figure 25 Comparison between RMS values of vibration signals at 5 Hz and 1 Nm.

For an operating frequency of 5 Hz, at no load the CoCrNi gears show less vibration than AISI 321. The percentage decrease in vibration is the highest in the Z-direction, 57 %, which is significant as it is also the axis that has vibrations generated due to the meshing of gears. This implies a smoother meshing between the gear teeth of CoCrNi. The trend remains similar with an increase in load to 0.5 Nm. A consistent decrease in vibration is found for the highest value of load, indicating the tendency of CoCrNi to 'settle in'with an increase in load.

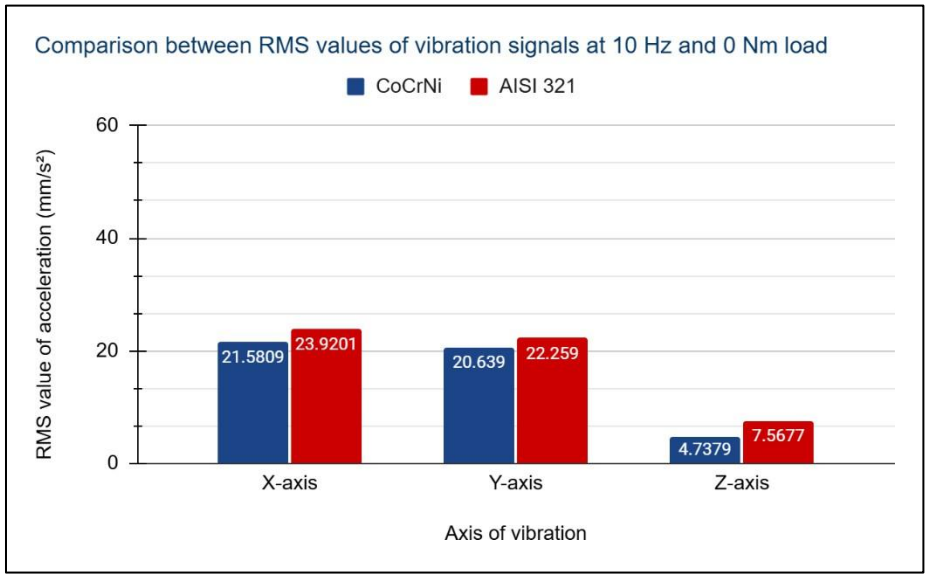

Figure 26 Comparison between RMS values of vibration signals at 10 Hz and 0 Nm.

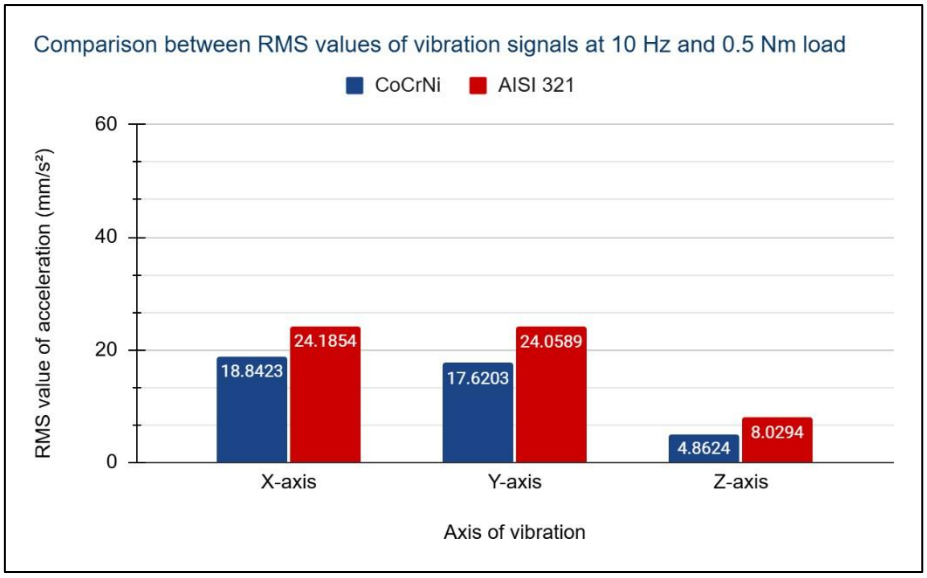

Figure 27 Comparison between RMS values of vibration signals at 10 Hz and 0.5 Nm.

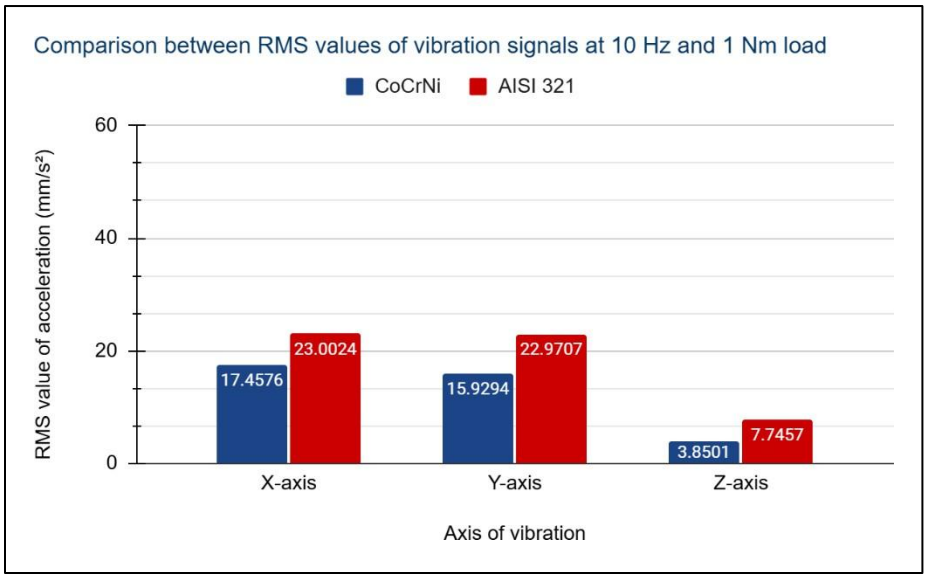

Figure 28 Comparison between RMS values of vibration signals at 10 Hz and 1 Nm.

Vibration RMS values show a decline in CoCrNi gears for an increase in operational frequency. Such characteristics prove promising in imparting a better fatigue life to the component. A decrease in radial and axial vibrations also means that it reduces the risk of flanking and thrust-induced bearing wear.

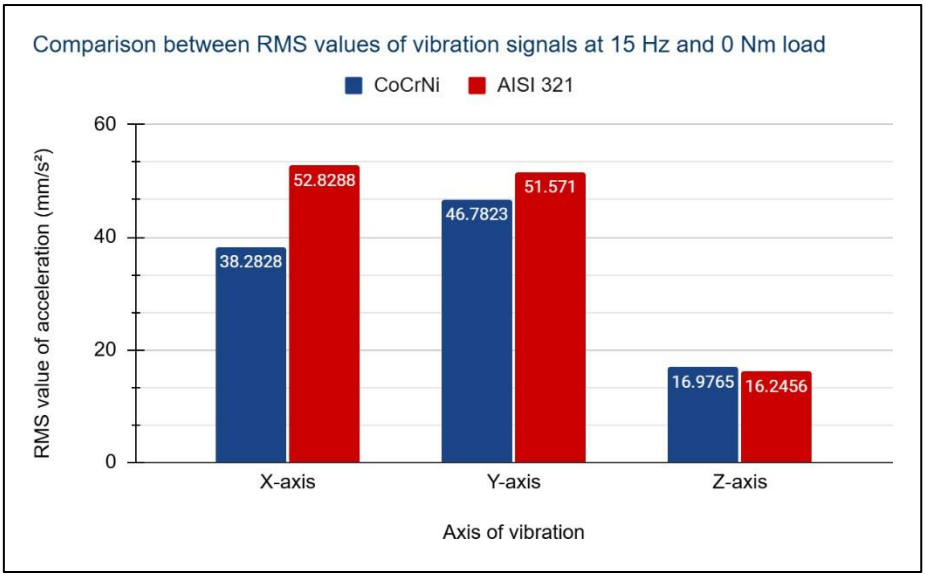

Figure 29 Comparison between RMS values of vibration signals at 15 Hz and 0 Nm.

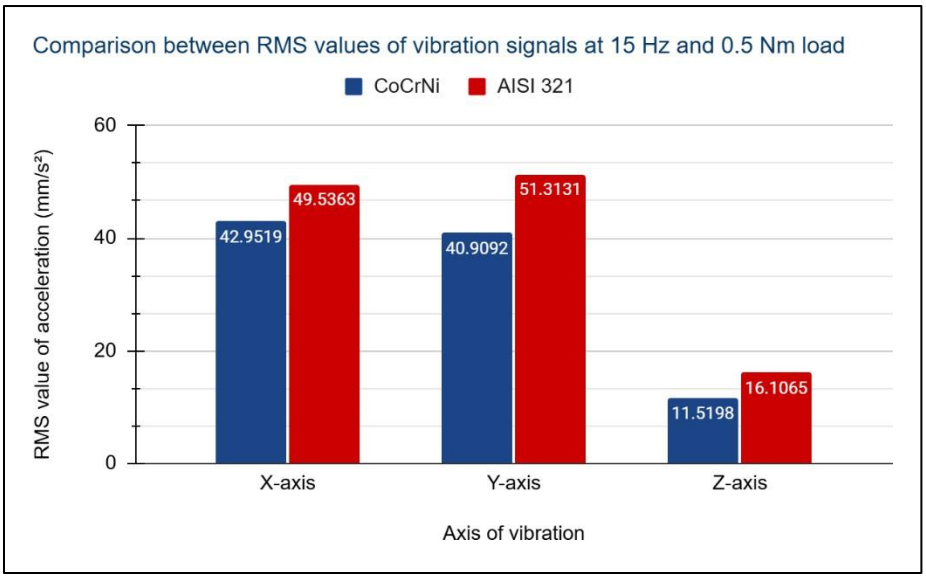

Figure 30 Comparison between RMS values of vibration signals at 15 Hz and 0.5 Nm.

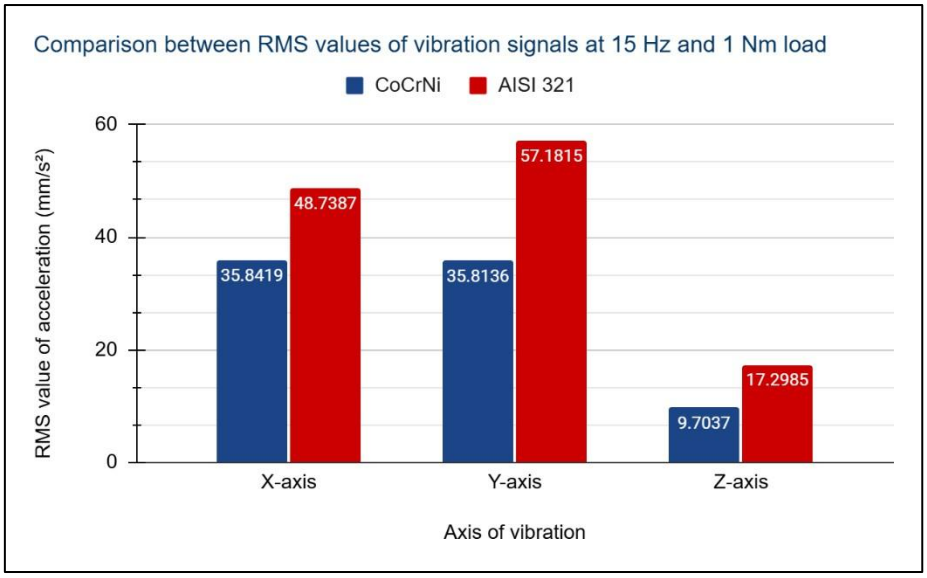

Figure 31 Comparison between RMS values of vibration signals at 15 Hz and 1 Nm.

While the tangential RMS for AISI 321 barely changes with an increase in load, for CoCrNi it drops by ≈ 7 mm/s^2 showing a non-linear damping behavior under higher loading. Axial vibration reduction is nearly half which further establishes that CoCrNi reduces thrust-related excitation that directly affects bearing fatigue. A summary of the observations from vibration RMS has been provided in the Table 5 for getting an overview briefly.

CoCrNi gears exhibit lower time-domain vibration levels than AISI-321 primarily because their intrinsic material properties both reduce the amplitude of each mesh impact and dissipate more of the resulting elastic energy before it propagates into the housing. First, CoCrNi has a notably higher elastic modulus (≈235 GPa) than AISI 321 (~195 GPa). When two teeth come into contact, a higher modulus means the contact zone deforms less, producing smaller force spikes. Those smaller spikes translate directly into lower accelerations measured for the gear body.

At the microscale, CoCrNi also dissipates more vibration energy internally. Its relatively low stacking-fault energy promotes the formation of coherent twin boundaries. As the gear teeth repeatedly engage, new twins and stacking faults form, which work-harden the

material and absorb additional energy that would otherwise contribute to elastic vibration.

In combination, these effects like stiffer tooth contacts, reduced energy transfer to the housing, enhanced internal friction via twinning, ongoing work-hardening, and grain-boundary scattering, ensure that CoCrNi gears generate and transmit significantly lower vibration amplitudes under identical operating conditions compared to AISI 321.

Table 5 Overview of vibration analysis results of CoCrNi versus AISI 321 gears.

Operating Conditions	**Vibration Acceleration RMS**		**% Decrease in vibration RMS**
	CoCrNi	***AISI 321***	
5 Hz and 0 Nm			
X-axis	5.3595	8.0553	33.46
Y-axis	6.4101	7.6422	16.12
Z-axis	1.347	3.1788	57.62
5 Hz and 0.5 Nm			
X-axis	5.0613	8.4184	39.87
Y-axis	7.5956	8.5019	10.65
Z-axis	1.7343	2.5188	31.14
5 Hz and 1 Nm			
X-axis	3.041	5.5731	45.43
Y-axis	3.7028	5.6491	34.45
Z-axis	1.0133	1.7592	42.39
10 Hz and 0 Nm			
X-axis	21.5809	23.9201	9.77
Y-axis	20.639	22.259	7.27
Z-axis	4.7379	7.5677	37.39
10 Hz and 0.5 Nm			

X-axis	18.8423	24.1854	22.09
Y-axis	17.6203	24.0589	26.76
Z-axis	4.8624	8.0294	39.44
10 Hz and 1 Nm			
X-axis	17.4576	23.0024	24.10
Y-axis	15.9294	22.9707	30.65
Z-axis	3.8501	7.7457	50.29
15 Hz and 0 Nm			
X-axis	38.2828	52.8288	27.53
Y-axis	46.7823	51.571	9.28
Z-axis	16.9765	16.2456	-4.49
15 Hz and 0.5 Nm			
X-axis	42.9519	49.5363	13.29
Y-axis	40.9092	51.3131	20.27
Z-axis	11.5198	16.1065	28.47
15 Hz and 1 Nm			
X-axis	35.8419	48.7387	26.46
Y-axis	35.8136	57.1815	37.36
Z-axis	9.7037	17.2985	43.90

Chapter 5 Conclusion and Scope for Future Work

This thesis set out to evaluate the suitability of equiatomic CoCrNi medium-entropy alloys (MEAs) as a gear material for demanding marine environments, comparing its performance against conventional austenitic and alloy steels such as AISI 316, 321, and 4140 which are conventionally marine grade steels. Key objectives included verifying the composition and microstructure of as-received CoCrNi ingot, assessing its tensile behavior and hardness, and conducting comparative vibration analyses of CoCrNi and AISI 321 gear pairs under controlled loading and speed conditions.

1. Mechanical properties characterization of CoCrNi show a strong work hardening and a uniformity in hardness post heat treatment. These properties surpass that of marine grade steel.
2. The reduction in vibration acceleration RMS along all three axes namely, axial, transverse, and tangential, is between 10 – 50% for different operating speeds and load conditions.
3. Taken together, the results demonstrate that CoCrNi (MEAs) combine an advantageous set of intrinsic material features like high stiffness, internal damping, and pronounced work-hardening, that yield measurably lower vibration amplitudes and offer compelling potential for marine-gear applications.
4. The reduction in the overall vibration strength of the signal also suggests that CoCrNi gears would be less prone to failure by fatigue. Their stable single phase FCC structure negates the possibility of inclusions that would otherwise act as crack nucleation sites.
5. It is important to note that CoCrNi can only be looked at as an alternative material to high strength gears where cost is not of concern. Critical applications where reliability, performance, and efficiency are the key considerations such as naval vehicles, military equipment, or aerospace systems, hold a strong potential in terms of application feasibility.

This study of CoCrNi gears can be expanded to include its fatigue life investigation against marine grade steels. As areas of application considering other properties of CoCrNi come forward, condition-based monitoring of such gears, coupled with in depth study of crack propagation in the teeth of such gears and its effect on gear vibrations can revolutionized research focused in structural applications of HEAs and MEAs. Giving a multidisciplinary perspective to this research, molecular dynamics simulations can be used to better justify the reasons behind the successful use of MEAs in demanding structural applications.

REFERENCES

[1] J. Wu, P. Wei, C. Zhu, P. Zhang, and H. Liu, “Development and application of high strength gears,” Jun. 01, 2024, *Springer Science and Business Media Deutschland GmbH*. doi: 10.1007/s00170-024-13479-x.

[2] G. I. Maitra, *Handbook of Gear Design*. New york: Marcel Dekker, 2006.

[3] V. Srivastava, D. Singh, A. G. Rao, and V. P. Deshmukh, “Root cause analysis of flywheel gear failure in a marine diesel engine,” *Eng Fail Anal*, vol. 156, Feb. 2024, doi: 10.1016/j.engfailanal.2023.107729.

[4] S. F. Hassan and M. R. Alam, “Failure analysis of gearbox and clutch shaft from a marine engine,” *Journal of Failure Analysis and Prevention*, vol. 10, no. 5, pp. 393–398, Oct. 2010, doi: 10.1007/s11668-010-9373-4.

[5] L. Hu, J. Yang, and Y. Yu, “Research on Vibration Diagnosis Method of Broken Tooth Failure for Marine High-Speed Gearbox,” in *Proceedings - 2020 5th International Conference on Smart Grid and Electrical Automation, ICSGEA 2020*, Institute of Electrical and Electronics Engineers Inc., Jun. 2020, pp. 153–157. doi: 10.1109/ICSGEA51094.2020.00040.

[6] J. Xu *et al.*, “Dynamic research on nonlinear vibration mechanism and control method for marine parallel propulsion system,” *Ocean Engineering*, vol. 323, Apr. 2025, doi: 10.1016/j.oceaneng.2025.120556.

[7] M. Fonte, L. Reis, and M. Freitas, “Failure analysis of a gear wheel of a marine azimuth thruster,” *Eng Fail Anal*, vol. 18, no. 7, pp. 1884–1888, Oct. 2011, doi: 10.1016/j.engfailanal.2011.07.009.

[8] F. D. C. Garcia Filho, R. O. Ritchie, M. A. Meyers, and S. N. Monteiro, “Cantor-derived medium-entropy alloys: bridging the gap between traditional metallic and high-entropy alloys,” *Journal of Materials Research and Technology*, vol. 17, pp. 1868–1895, Mar. 2022, doi: 10.1016/j.jmrt.2022.01.118.

[9] S. Zhao, G. M. Stocks, and Y. Zhang, “Stacking fault energies of face-centered cubic concentrated solid solution alloys,” *Acta Mater*, vol. 134, pp. 334–345, Aug. 2017, doi: 10.1016/j.actamat.2017.05.001.

[10] M. Yang, D. Yan, F. Yuan, P. Jiang, E. Ma, and X. Wu, “Dynamically reinforced heterogeneous grain structure prolongs ductility in a

medium-entropy alloy with gigapascal yield strength," *Proc Natl Acad Sci U S A*, vol. 115, no. 28, pp. 7224–7229, Jul. 2018, doi: 10.1073/pnas.1807817115.

[11] D. Hua *et al.*, "Atomistic insights into the deformation mechanism of a CoCrNi medium entropy alloy under nanoindentation," *Int J Plast*, vol. 142, Jul. 2021, doi: 10.1016/j.ijplas.2021.102997.

[12] Z. Pang *et al.*, "Electrosynthesis and Evaluation of Homogeneous CoCrNi Medium-Entropy Alloys for Structural Applications," *Metallurgical and Materials Transactions B: Process Metallurgy and Materials Processing Science*, vol. 54, no. 5, pp. 2824–2839, Oct. 2023, doi: 10.1007/s11663-023-02877-3.

[13] D. Liu *et al.*, "Exceptional fracture toughness of CrCoNi-based medium-and high-entropy alloys close to liquid helium temperatures."

[14] L. MatWeb, "MatWeb – The Online Materials Information Resource." Accessed: Jun. 03, 2025. [Online]. Available: https://www.matweb.com/search/DataSheet.aspx?MatGUID=dfced4f11d63459e8ef8733d1c7c1ad2

[15] L. United Performance Materials, "United Performance Materials – High-Performance Material Solutions." Accessed: Jun. 03, 2025. [Online]. Available: https://www.upmet.com/sites/default/files/datasheets/321.pdf

[16] P. K. Arya, N. K. Jain, and D. Sathiaraj, "Microstructure and mechanical properties of additively manufactured Ti6Al4VxCryNi alloy," *CIRP J Manuf Sci Technol*, vol. 53, pp. 67–80, Oct. 2024, doi: 10.1016/j.cirpj.2024.07.001.

[17] G. Laplanche, A. Kostka, C. Reinhart, J. Hunfeld, G. Eggeler, and E. P. George, "Reasons for the superior mechanical properties of medium-entropy CrCoNi compared to high-entropy CrMnFeCoNi," *Acta Mater*, vol. 128, pp. 292–303, Apr. 2017, doi: 10.1016/j.actamat.2017.02.036.

[18] G. Bracq *et al.*, "Combining experiments and modeling to explore the solid solution strengthening of high and medium entropy alloys," *Acta Mater*, vol. 177, pp. 266–279, Sep. 2019, doi: 10.1016/j.actamat.2019.06.050.

[19] Z. Zhang *et al.*, "Dislocation mechanisms and 3D twin architectures generate exceptional strength-ductility-toughness combination in CrCoNi medium-entropy alloy," *Nat Commun*, vol. 8, Feb. 2017, doi: 10.1038/ncomms14390.

[20] W. Zhang, P. K. Liaw, and Y. Zhang, “Science and technology in high-entropy alloys,” Jan. 01, 2018, *Science China Press*. doi: 10.1007/s40843-017-9195-8.

[21] X. Gao *et al.*, “High-entropy alloys: a review of mechanical properties and deformation mechanisms at cryogenic temperatures,” Mar. 01, 2022, *Springer*. doi: 10.1007/s10853-022-07066-2.

[22] E. P. George, W. A. Curtin, and C. C. Tasan, “High entropy alloys: A focused review of mechanical properties and deformation mechanisms,” Apr. 15, 2020, *Acta Materialia Inc*. doi: 10.1016/j.actamat.2019.12.015.

[23] J. D. . Smith, *Gear noise and vibration* . Marcel Dekker, 2003.